Bioresource Technology 318 (2020) 124263

Contents lists available at ScienceDirect

Bioresource Technology

journal homepage: www.elsevier.com/locate/biortech

Hydrothermal processing of a green seaweed *Ulva* sp. for the production of monosaccharides, polyhydroxyalkanoates, and hydrochar

Efraim Steinbruch [a,b], Dusan Drabik [c], Michael Epstein [a], Supratim Ghosh [a], Meghanath S. Prabhu [a], Michael Gozin [d], Abraham Kribus [b], Alexander Golberg [a,*]

[a] Porter School of Environment and Earth Sciences, Tel Aviv University, Tel Aviv, Israel
[b] School of Mechanical Engineering, Tel Aviv University, Tel Aviv, Israel
[c] Agricultural Economics and Rural Policy Group, Wageningen University, Wageningen, the Netherlands
[d] School of Chemistry, Tel Aviv University, Tel Aviv, Israel

HIGHLIGHTS

- Hydrothermal processing of the whole *Ulva* sp. biomass vs. extracted carbohydrate fractions of starch and cellulose.
- Glucose is a major released monosaccharide with hydrothermal deconstruction.
- Most of the glucose is released from starch.
- Whole biomass hydrolysis preferred for PHA fermentation with *Haloferax mediterranei.*
- The highest ash-free hydrochar yield was from *Ulva* cellulose.

ARTICLE INFO

Keywords:
Biofuel
Polyhydroxyalkanoates
Seaweed
Ulva sp.
Biorefinery
Subcritical hydrolysis
Hydrochar
Glucose
Marine starch
Cellulose
Economic analysis

ABSTRACT

In the fermentation and bioenergy industry, terrestrial biomass is usually fractionated and the collected components, such as starch, are processed separately. Such a separation has not been reported for seaweeds. In this work, the direct hydrothermal processing of the whole green seaweed *Ulva* sp. biomass is compared to processing of separated starch and cellulose, to find the preferable route for monosaccharide, hydrochar, and polyhydroxyalkanoates (PHA) production. Glucose was the major released monosaccharide. A significant share of the glucose yield comes from the starch fraction. The highest hydrochar yield with the lowest ash content was obtained from the separated cellulose fraction. The highest PHA yield was obtained using a whole *Ulva* sp. hydrolysate fermentation with *Haloferax mediterranei*. Economic analysis shows the advantage of direct *Ulva* sp. biomass fermentation to PHA. The co-production of glucose and hydrochar does not add significant economic benefits to the process under plausible prices of the two outputs.

1. Introduction

Seaweeds, which are ranked among the most efficient photosynthetic organisms on earth, and do not compete for land or potable water with food crops, can provide a sustainable alternative source of biomass for biofuel. However, the use of seaweed as feedstock, enabling processing technologies, and sustainable development are still in their early stage and require technological platforms for cultivation and energy conversion. An important step in seaweed biomass conversion to biofuel is the de-polymerization of the polysaccharides to produce monosaccharides. These monosaccharides can be used, for example, as sources for bioethanol via fermentation.

The traditional practice of food and biomass processing, including the processing of major crops like potato, corn, soy, and rice, involves the disintegration of the initial biomass followed by its separation to the main components such as starch, cellulose, proteins, oils, and fibers. Such separation results in more pure streams with concentrated components that are than used as ingredients and raw materials for multiple downstream processes including fermentation. For example, starch is a common feedstock for ethanol fermentation and oils and starch are used

* Corresponding author.
E-mail address: agolberg@tauex.tau.ac.il (A. Golberg).

https://doi.org/10.1016/j.biortech.2020.124263
Received 11 September 2020; Received in revised form 9 October 2020; Accepted 11 October 2020
Available online 16 October 2020

for polyhydroxyalkanoates (PHA) production (Chien and Ho, 2008; Kahar et al., 2004). This major ingredient separation, however, is not a common practice in seaweed biomass processing. Although traditional large-scale seaweed processing industry focuses on the separation of hydrocolloids such as alginate, carrageenan, and agarose from the rest of the biomass, most of the works published till now focused on the whole seaweed biomass deconstruction and fermentation (Khambhaty et al., 2012) with only a few works comparing the yield of fermentation of separated streams (Hargreaves et al., 2013).

Green macroalgae such as *Ulva* sp. have been investigated and proposed as a feedstock for saccharification and fermentation in multiple previous studies (El-Sayed et al., 2016; Ghosh et al., 2019; Korzen et al., 2015). However, to the best of our knowledge, the separation of major components before the follow-up fermentation has not been reported, and all the reports focused on the processing of the whole biomass (Ghosh et al., 2019; Zollmann et al., 2019). In the two recent works, we have developed protocols for the fractionation of the *Ulva* sp. biomass into major components such as starch, cellulose, proteins, and ulvan (Prabhu et al., 2019a, 2020). The goal of this study is to compare the release of fermentable monosaccharides, production of PHA and hydrochar using subcritical water hydrolysis for the two options: the whole *Ulva* sp. biomass vs. the processing of separate starch granules from *Ulva* sp. (US) and cellulose from *Ulva* sp. (UC), under the same process parameters.

Currently, technologies to produce monosaccharides from the whole biomass and its polysaccharides on a commercial scale rely on thermochemical and enzymatic processes. However, the technologies which require enzymes are expensive (Klein-Marcuschamer et al., 2012) and catalysts such as acids are environmental hazards that require additional treatments (Jiang et al., 2016). In contrast, the subcritical hydrothermal process using water (liquid water at temperatures of 100-374ºC) as a solvent and as a catalyst, does not involve any addition of chemicals and therefore it can potentially serve as a sustainable process for biomass deconstruction. This process is inherently suitable for seaweed biomass that already contains a high fraction of water (85%), and thus saves the need for drying that can be expensive both economically and energetically (Möller et al., 2011). Several studies have been conducted on the subcritical water hydrolysis of the whole seaweed biomass (Meillisa et al., 2015; Rodrigues et al., 2015).

The hydrothermal deconstruction of seaweed biomass produces a variety of small organic molecules, which can be used as a carbon source for fermentation to produce not only ethanol but also other products. AS an example is the PHA that can be used to produce degradable industrial polymers ('bioplastics') that may substitute the conventional polymers derived from fossil fuels, as a part of a green economy. PHA production using carbon source from the whole *Ulva* sp. subcritical water hydrolysates is described in (Ghosh et al., 2019).

Furthermore, the subcritical water hydrolysis process at the range of 180-260ºC also leads to hydrothermal carbonization of seaweed biomass. In this process, the carbon fraction in the solid residue (hydrochar) is increased due to the release of water molecules from carbohydrates, thus leading to an increase in the residue's calorific value, which makes it more suitable for combustion as a solid fuel than untreated biomass (Greiserman et al., 2019; Hoekman et al., 2011). Although previous works studied the properties of hydrochar from *Ulva* and other seaweeds (Greiserman et al., 2019; Kantarli et al., 2019) to the best of our knowledge, there are no reports on hydrochar produced from starch and cellulose separated from the algal biomass.

To further advance the processing of green seaweed biomass to biofuels and bioplastics, in this work, for the first time, we compare the production yields and economics of monosaccharides, PHA, and hydrochar from separated major carbohydrates of *Ulva* sp. biomass vs. their production from the whole algae. Our results show that extracting first the starch fraction from the whole seaweed is the better way for releasing the glucose, while the whole seaweed biomass treatment is preferred for PHA and cellulose is the best for hydrochar production. Preliminary economic analysis shows the advantage of direct whole Ulva sp biomass conversion to PHA without co-production of glucose and hydrochar.

2. Materials and methods

2.1. *Ulva sp. Biomass cultivation*

Green marine seaweed *Ulva* sp. was cultivated at the Israel Oceanographic and Limnological Research (IOLR Ltd., Haifa, Israel), under controlled conditions using 40 L and 1000 L outdoor tanks with aeration and supplied with running natural Mediterranean seawater. During the cultivation in the 40 L tanks, the seaweeds were fertilized once a week, with 0.06 mM NaH_2PO_4 and 0.59 mM NH_4Cl (Haifa Chemicals Ltd., Israel). After 4 weeks of cultivation (from October to November 2018), the biomass was harvested, washed with seawater, and drained with a spinner. This biomass, defined as the wet weight (WW), was used for the starch and cellulose extraction. For the sake of accurate calculation of the conversion yields, the results are reported relative to the algae dry weight (DW), obtained by drying the fresh seaweed at 40 °C until constant weight.

2.2. *Extraction and purification of starch granules from Ulva sp. biomass.*

After washing and spinning, the biomass (7 kg WW of *Ulva* sp. biomass) was homogenized in the cold distilled water (1:20 (w/v)) (HG-300, Hasigtai Machinery Industry Co., Ltd., Taiwan). The slurry was separated to liquids and solids with a nylon filter with 100 μm, 50 and 10 μm pore size nylon filters. The filtrate after 100 μm filtration was collected for cellulose extraction. The filtrate after 50 and 10 μm filtration was centrifuged for 6 min (Rotanta, 46RSC, Hettich Instruments, LP, Germany), to obtain a pellet containing the starch granules. To remove pigments and lipid, the pellet was washed three times with absolute ethanol (19.8 L). The white pellet was dried at room temperature for 24 h.

2.3. *Extraction and purification of cellulose from Ulva sp. (UC)*

1,500 gr of the particles, after 100 μm filtration as described above, were bleached with 540 gr of $NaClO_2$, in 1.5 L acetic buffer (Sigma-Aldrich, Israel). The mixture was diluted with distilled water to 15 L, poured into glass bottles, and heated for 8 h at 60ºC. The product was neutralized (pH ~7), as indicated by the coloration of a paper indicator, and then filtered. 9 L of 0.5 M NaOH was added to the remaining solid residue and heated at 60ºC overnight. The obtained material was washed with distilled water until neutrality (pH ~7), as indicated by the coloration of a paper indicator, and dried at room temperature. Three L of 5% HCL was added to the obtained resultant, and the suspension was heated till boiling. Once boiling was reached, the heating was stopped, and the slurry was left to cool overnight. The residue was washed until neutrality (pH ~7, paper indicator), filtered, and dried at room temperature for 24 h before being used for further experiments.

2.4. *Subcritical water hydrolysis*

A batch experimental system, described in details in (Greiserman et al., 2019), was used for the subcritical biomass hydrolysis. In brief, the system consists of a 0.25-liter batch reactor (Zhengzhou Keda Machinery and Instrument Equipment CJF-0.25, China) heated by an electric heater. The temperature is measured with an MRC TM-5005 digital temperature gauge using 1/16″ thermocouple type K (Watlow, USA). The pressure was constantly measured using the MRC PS-9302 pressure gauge monitored with the MRC PS100-50BAR. A magnetic coupling drive was used to mix the slurry inside the pressure reactor (in all experiments, the stirrer was set at 70 RPM). The magnet coupling is cooled (20ºC) using a chiller (Guangzhou Teyu Electromechanical Co., Ltd Cw-

5200ai, China). For sampling, the passes through a condenser (also cooled by the chiller) and a cold trap (20ºC) before entering the sampling tube. The cooling water is circulated from a chiller. The air is evacuated from the reactor before starting each experiment with the vacuum pump (MRC ST-85). The final hydrolysate was separated into liquid and solid phases by centrifugation, 7,000 RPM for 3 min (Rotanta 46 RSC, Hettich Instruments, LP, Germany). The hydrothermal treatment experiments were conducted under process conditions similar to the previous studies (Choi et al., 2013; Meillisa et al., 2015): temperature 180ºC, 220ºC, and 260ºC; residence time 10 min, 20 min, and 40 min; 100% seawater (salinity of 38.2 gr/L); and 8% (w/w) solid load (8 gr biomass DW in 92 mL of seawater). Each test was repeated twice.

2.5. Ion chromatography for the analysis of monosaccharides and glucuronic acid

Monosaccharides were determined using high-pressure ion chromatography (HPIC) (Dionex ICS-5000, Dionex, Thermo Fischer Scientific, MA, USA) using a Dionex™ AminoPac™ PA10 IC analytical column with its corresponding guard column (Thermo Fischer Scientific, UK). The voltage waveform "Carbohydrates (Standard quad)" was used. The autosampler containing the diluted sample and the standards was kept at 5 °C. The phase flow rate was 0.25 mL/min, and the column temperature was set to 30 °C. The identification and quantification of monosaccharides in the HTC hydrolysates were performed by comparison with reference standards of fructose, xylose, glucose, galactose, rhamnose and glucuronic acid (Sigma-Aldrich, Saint-Louis, USA) stabilized with water (TCI America™). The calibration curves of the monosaccharides and glucuronic acid were in the range of 22–0.21 μg/mL. Before analysis, the HTC hydrolysates samples were diluted with ultrapure water (50/150 times) and filtered with 0.22 μm syringe-filter (Millipore, USA) into HPIC vials (Thermo Fischer Scientific, USA).

2.6. The mass balance of the hydrolysate products.

For the calculation of mass balance, the hydrolysate (H) was dried at 40 °C resulting in the solid matter (Z) that contained hydrochar, salts, and soluble solids. The mass of the evaporated water (E) was measured gravimetrically. Secondly, the liquid phase (X) of the hydrolysate was sampled and dried at 40 °C (the mass of evaporated liquid (K) was measured gravimetrically as above). The resulting solid (T) contained salts and water-soluble organic matter. The total soluble solids (S) are calculated for the total hydrolysate volume. As the % salinity in the experiments is known, the Total Soluble ash-free solids (AFS) can be calculated as follows:

$$H = Hydrochar + E + T$$

$$T = X\text{-}K$$

$$S = (T/X)\cdot(X + E)$$

$$AFS = S\text{-}(E + K)\cdot\%Salinity$$

$$Hydrochar = Z\text{-}S\text{-}salts$$

2.7. Elemental and caloric value analyses

Elemental analysis (CHNS) was done using ThermoScientific CHNS Analyzer (Flash2000) at the Technion (Israel Institute of Technology, Haifa) Department of Chemistry Service Unit. The oxygen atom content was determined by the balance as follows:

$$\%O = 100\%\text{-}(\%C + \%H + \%N + \%S + \%Ash) \quad (2)$$

For caloric value and ash analysis, 1 g of untreated algae and residual carbonized material was dried at 40 °C to constant weight and were analyzed for energy content as High Heating Value (HHV) according to ASTM D5865 -13 (Standard Test Method for Gross Calorific Value of Coal and Coke) and for ash according to D5142 standard. The adjusted HHV (same ash content as initial biomass) was calculated for the hydrochar according to:

$$Adjusted\ HHV = HHV \cdot \left(\frac{1 - (\%\ ash\ untreated\ Ulva/100)}{1 - (\%\ ash\ hydrochar/100)} \right) \quad (3)$$

2.8. The high heating value of the residue and moisture content

For residue and moisture analysis, untreated seaweed, starch, cellulose, and hydrochar were dried at 40 °C to constant weight and analyzed. For energy content (HHV) a Parr 6200 Calorimeter was used according to ASTM D5865-13 standards. Ash and moisture content was analyzed according to the D5142 standard.

For validation of the results obtained, the HHV was also estimated using the following two correlations:

(Boie, 1953):

$$Q = 151.2C + 499.77H + 45S - 47.7O + 27N \quad (4)$$

(Grummel and Davies, 1933):

$$Q = \left[\frac{654.3H}{(100 - A)} + 424.62 \right] \cdot \left[\frac{C}{3} + H - \frac{O}{8} + \frac{S}{8} \right] \quad (5)$$

Where Q is the high heating value (MJ kg^{-1}), C, H, N, S, O, A is the weight percentage of carbon, hydrogen, nitrogen, sulfur, oxygen, and ash, respectively.

2.9. Starch content analysis

The starch content was determined using a total starch assay kit (K-TSTA-100A, Megazyme, Ireland). Three samples of 10 mg DW Ulva biomass, grounded to a fine powder using a mortar and pestle after freezing with liquid N_2, were washed twice in 200 μL, 80% (v/v) ethanol to remove glucose. Two hundred microliters of 2 M potassium hydroxide were then added to the tubes incubated horizontally for 30 min at 37 °C and 150 rpm. Next, the mixture was heated in a boiling water bath for 1 min to dissolve the starch. The tubes were cooled at 23 °C for 5 min. Then 0.8 mL sodium acetate buffer (1.2 M, pH 3.8) was added. Next, 0.01 mL α-amylase and 0.01 mL amyloglucosidase was added and mixed using a vortex. The mixture was incubated for 1.5 h at 50 °C and 150 rpm. Following the incubation, the tubes were centrifuged at 1800 g for 10 min (Eppendorf centrifuge 5424, Hamburg). The released glucose was measured at 510 nm (Tecan Infinite 200 Pro Spectrophotometer, Tecan Inc, Switzerland) after reacting 0.01 mL from the supernatant with 0.3 mL glucose oxidase–peroxidase (GODPOD) for 20 min. The starch concentration was calculated taking the molar mass conversion from glucose to amyhydroglucose.

2.10. Polyhydroxyalkanoates production by Haloferax mediterranei

Wild-type *Haloferax mediterranei* strain was grown in rich medium (Hv-YPC) containing (per L) 144 g of NaCl, 21 g of $MgSO_4{\cdot}7H_2O$, 18 g of $MgCl_2{\cdot}6H_2O$, 4.2 g of KCl, and 12 mM Tris HCl buffer (pH 7.5). The culture was kindly provided by Prof. Uri Gophna, Faculty of Life Sciences, Tel Aviv University. For the cultivation solid media, agar (Difco, USA) was added at a concentration of 15 g per L and was dissolved by heating the medium in a microwave oven. Yeast extract (0.5% w/v; Difco, USA), 0.1% (w/v) peptone (Oxoid) (Difco, USA), and 0.1% (w/v) Casamino Acids (Difco, USA) was added and the medium was autoclaved. After cooling, $CaCl_2$ was added to a final concentration of 3 mM. For the preparation of culture plates, 2% w/v of Agar powder was added to the medium. The organism was grown at 42 °C in a temperature-controlled incubator. For liquid cultures, the microorganism was grown in 250 mL Duran bottles with a working volume of 100 mL. The culture was grown in a shaking incubator (MRC Labs, Israel) at 42 °C with a rotational speed of 180 rpm. The media pH was adjusted to 7.2.

The cell suspension (1 mL) was centrifuged at 12,000 g for 5 min and the pellet was suspended in 1 mL of distilled water. Subsequently, 40 μL of Nile Red (Sigma) (80 μg•mL-1 dissolved in dimethyl sulfoxide (DMSO) was added to the suspension to give a final concentration of 3.1 μg Nile Red per mL suspension and was incubated at room temperature for 30 min. The stained suspension was then centrifuged at 12,000 g for 5 min, and the supernatant was discarded. Distilled water (1 mL) was added, and the resulting pellet was vigorously vortexed. An aliquot of the suspension was pipetted into a 96-well microplate. The fluorescence was then read at excitation and emission wavelength 535 and 605 nm, respectively, using a Multilabel Plate Reader (Tecan, Switzerland). A standard curve was plotted for fluorescence intensity versus polyhydroxyalkanoates (PHA) concentration with known concentrations of PHA. The unknown amount of PHA was determined from the standard curve with two repeats per point.

The yield of PHA was determined by a gravimetric method wherein the extracted polymer was dried at 70 °C till constant weight was obtained. The yield (%) was calculated as in (Ghosh et al., 2019):

$$Yield = \frac{w_{PHA}}{w_{cell}} \times 100 \quad (6)$$

Where w_{PHA}(g) is the amount of PHA recovered from dry cell weight w_{cell}(g). The PHA produce yield was also calculated per gram of solid loading biomass (g PHA/g dry *Ulva sp.*).

2.11. Microscopic studies.

Dry *Ulva* sp. biomass, dry starch from *Ulva* (US), dry cellulose from *Ulva* (UC), and its hydrochars were studied for their morphology using transmission electron microscopy. Surface morphology was observed using scanning electron microscopy (SEM). SEM image was obtained using Quanta 200 (FEG ESEM, Oregon, USA) after fixing the sample on silicon tape and then coating with gold using a sputter coater.

2.12. Fourier-transform infrared spectroscopy

FT-IR spectra of vacuum-dried *Ulva* biomass, US, UC, and corresponding biochar samples were measured in the spectral range of 4000–400 cm^{-1} (at 4 cm^{-1} resolution) using Bruker Tensor 27 FT-IR spectrophotometer, equipped with standard Pike ATR attachment.

2.13. Thermogravimetric and differential scanning calorimetry

Thermogravimetric and differential scanning calorimetric (TG-DSC) analyses were carried out to study the thermal properties of vacuum-dried *Ulva* biomass, US, UC, using a Jupiter STA 449 F5 instrument (NETZSCH, Germany). Dry powder (5 mg) was exposed to a temperature in range of 30–900 °C with the increase in temperature of 10 °C/min under nitrogen (N_2) atmosphere. An empty crucible was used as the reference. Thermal analysis of US was compared with that of standard potato starch (Sigma-Aldrich, 33615). To study the gelatinization temperature of the whole *Ulva* sp., US and UC, DSC was performed following the procedure of Malumba et al. (2017). In brief, the dry powder (2.5 mg DW) was weighed into an aluminum crucible, and deionized water (7.5 μL) was added. The crucibles with the slurry were hermetically sealed with a lid having a hole in the center. After one hour of storage at room temperature for equilibration, measurements were performed over the temperature range of 30 to 200 °C. Samples were scanned at a temperature increase rate of 10 °C/min., under N_2 against empty crucibles as a reference. Thermal parameters of gelatinization, including onset (To), peak (Tp), conclusion (Tc) temperatures, gelatinization range (ΔT), and gelatinization enthalpy (ΔH) were recorded. The onset temperature and peak temperatures were computed using NETZSCH Proteus Thermal analysis software (NETZSCH, Germany). ΔH was calculated by dividing the integrated peak area with heating temperature rate (K/s) and further with the weight (mg).

2.14. Statistical analysis

All samples were hydrolyzed in duplicates, and each hydrolysate was injected twice for HPIC analysis. Data were reported as the mean weight fraction of the product per g of biomass (mg of product g^{-1} DW (Dry Weight) biomass) ± standard deviation. Statistical analysis was performed with Excel (ver. 13, Microsoft, WA) and data analysis package and R-studio (R-studio: an integrated development environment for R (Version 1.1.383) Boston, MA).

3. Results and discussion

3.1. Dry mass and ash content in Ulva sp. Biomass

Dewatered, fresh *Ulva sp*. biomass was characterized by dry mass and ash content. The dry matter weight content (dried at 40 °C) was 15.4 ± 1.3 (%w/wet weight) and ash content was 28.4 ± 0.8 (%w/DW).

3.2. Ulva starch granules extraction and characterization.

The *Ulva* sp. biomass showed 5.7 ± 0.32 (%w/DW) starch content when analyzed using the Megazyme total starch assay kit. The process followed for native starch granules extraction from *Ulva* sp. (US). This procedure can be scaled up for application in a biorefinery process for the commercial recovery of the US. Starch granules, observed with SEM, mostly resembling a sphere, but other shapes such as pear-shaped, and some irregularly shaped granules were also observed. The extraction of starch was prepared from 7 kg fresh *Ulva* sp., (DM of 15%). All the fractions of US obtained at the end were dried at 105 °C and gravimetrically weighed for quantification. The US granules weight obtained after centrifugation and drying was 4.9% of the *Ulva* DW. The extracted fraction of starch granules showed 68.8 ± 1.64%w starch content when analyzed using Megazyme total starch assay kit, corresponding to 59 ± 1.5% starch extraction yield (out of the potentially extractable starch content). The purity of US is close to the purity of various other commercial sources of starches such as from rice (73–87%) or potato (68–79%)(Prabhu et al., 2019b). The ash content of the fractions of starch was 3.8 ± 0.54% (w/w).

The FTIR spectroscopy patterns can be used to understand the chemical bonding and short-range molecular order of starches. The O–H stretching vibration in US and potato starch (PS) samples is found to be a broad-band with a peak position at 3300 cm^{-1}. Such broad nature of the peak indicates that the starch is having strong hydrogen bonding interaction among themselves as well as with the water molecules present in it. All the peaks in the fingerprint region of starches (between 1500 and 400 cm^{-1}) were observed for both starches. Attenuated Total Reflectance-FTIR spectra of US and PS showed remarkable similarity in absorption pattern. The absorption peaks in the region 1100–900 cm^{-1} have shown to be sensitive to variation in starch structure, providing a notion about the crystalline and the amorphous regions in starch (Warren et al., 2016). The higher absorbance ratio of 1036 cm^{-1} in the US indicated that the US has a higher amount of amorphous region as compared with PS, which shows a resemblance to a previous study reported in ref (Prabhu et al., 2019a).

Thermogravimetric analysis monitors the thermally-induced changes of a compound during heating. The TGA curve showed loss of mass from the starch sample at rising temperatures. Under non-oxidative degradation, a mass loss of 4.9 ± 0.15% from 30 °C to 100 °C was recorded. Between 100 °C and 314 °C, 55.8 ± 1.35% mass loss was observed, and 10.4 ± 0.25% mass loss occurred between 314 °C and 640 °C. The initial weight loss observed in the starch TGA curve can be attributed to the loss of residual moisture at a temperature range of 40–100 °C(Le Corre et al., 2010). The actual starch decomposition started at a temperature of 284 °C and most of the starch decomposed at 298 °C.

Structural features of starch granules influence their thermal-

degradation during combustion. In the DCS curve the endothermic peak of the thermal phase transition was observed at 64 °C. This peak temperature is the melting phase transition point of US from a solid crystalline state to an amorphous molten state, following the vaporization of the moisture content at higher temperatures. This pattern of degradation of US observed by TGA and DSC shows similarity to that of PS (Rodrigues et al., 2015).

3.3. *Ulva* cellulose extraction and characterization.

The fraction of cellulose (UC) obtained after centrifugation and drying was 7.6 ± 0.23%w/w of the *Ulva* DW. SEM of the UC revealed a typical web-like structure composed of numerous intertwined cellulose "threads". The FTIR spectroscopy patterns can be used to understand the chemical bonding and short-range molecular order of cellulose. Characteristic functional groups include O–H stretching at 3331 cm^{-1}. Such broad nature of the peak indicates that the cellulose has strong hydrogen bonding interaction among its threads. The peaks in the fingerprint region of celluloses, H-C–H group at 1427 cm^{-1}, and C-O-C group at 1025 cm^{-1} were observed. According to the analysis (FTIR), it is possible to determine that cellulose was indeed obtained, but it is not possible to determine the degree of purity.

TGA showed thermally-induced changes in the UC, during heating. The thermal degradation pattern is affected by structural features such as the nature of crystallinity, molecular weight, and orientation. The TGA curve reveals the loss of mass from the UC sample at rising temperatures. Under non-oxidative degradation, a mass loss that starts below 100 °C is probably due to the vaporization of moisture absorbed by UC. Mass loss of 27 ± 0.7% was recorded from 280 °C to 337 °C. Between 471 °C and 605 °C, 11.8 ± 0.38% mass loss was observed. The UC decomposition started at a temperature of 280 °C, and most of the UC is decomposed at 337 °C. This pattern of degradation of UC observed by TGA shows similarity to that of microcrystalline cellulose (Acros Organics™, CAS Number: 9004–34-6, Sigma, IL). The temperature ranges of mass losses detected in TGA thermograms are well correlated with the exothermic peaks observed in the corresponding DSC thermograms. Under the oxidizing air atmosphere, the exothermic peaks (319 °C, 542 °C) could be attributed to the thermal oxidation of the UC.

3.4. Monosaccharide release under subcritical water hydrolysis

The pressure measured during the experiment is close to the theoretical vapor pressure of water at the measured temperature, meaning that no other gases were formed during the experiment. The reactor is warming up slowly with 30 min of heating time to reach a temperature of 150 °C (5 °C/min). The reactor cooling duration was 125–180 min until it reached room temperature. The pH of the hydrolysates was 4.45 ± 0.31.

Glucose was the major released monosaccharide from *Ulva* sp. under the tested conditions. The maximum average yield achieved was 16.1±0.8 mg glucose/g dry *Ulva sp.*, at 180 °C for 40 min treatment time. The dependence of the yield on reaction temperature and residence time is shown in Fig. 1. Glucose yield was highest at 180 °C and decreased at higher temperatures. Temperature (p-val < $2 \cdot 10^{-5}$), retention time (p-val < 0.003) and their combination (p-val < 0.001) are significant in glucose release from the whole biomass. As described previously (Choi et al., 2013), in the subcritical condition, monosaccharides are depolymerized into other byproduct compounds, and

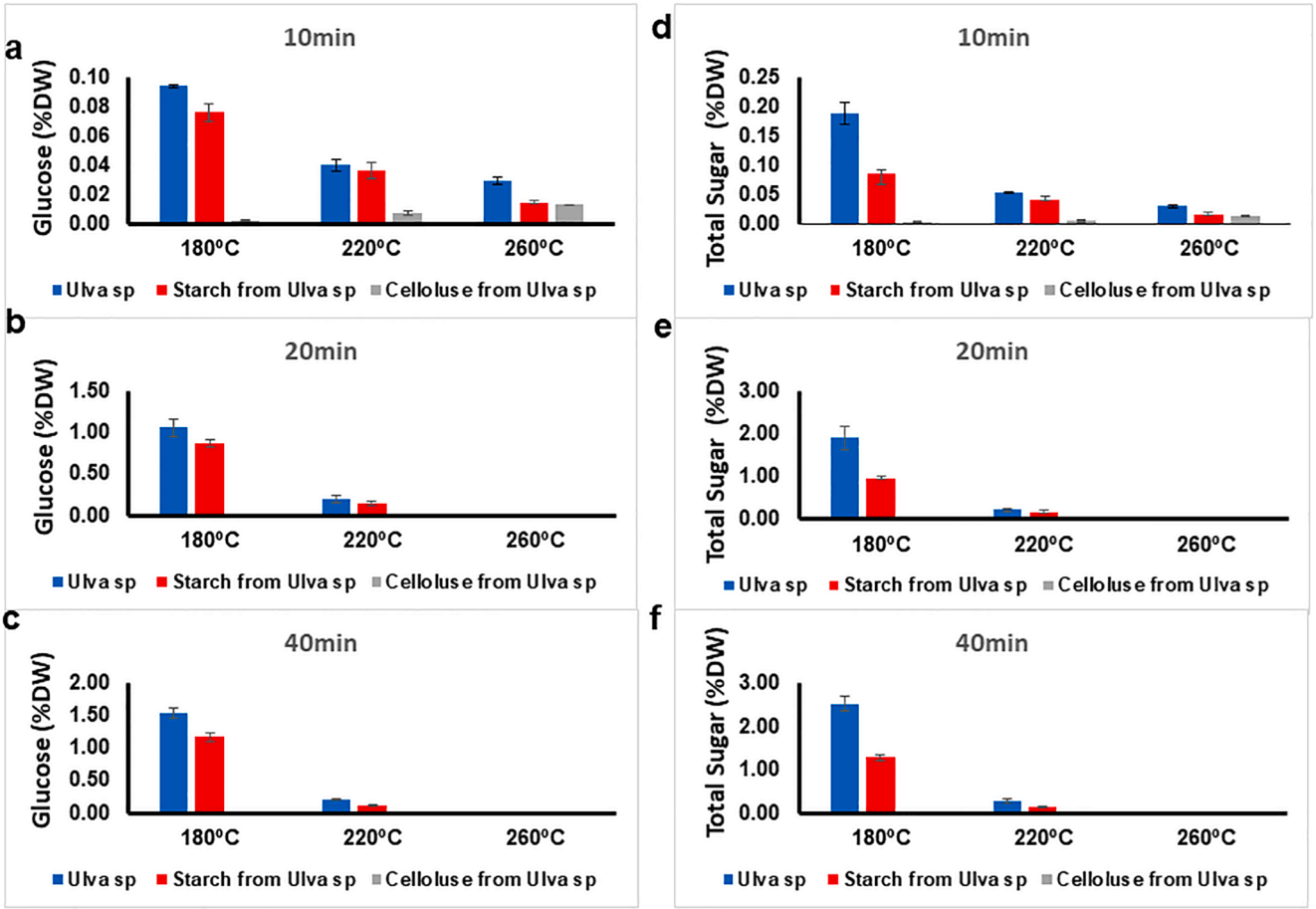

Fig. 1. Dynamics of glucose release. a. 10 min, b. 20 min, c.40 min residence time. Total sugar yield. d. 10 min, e. 20 min, f.40 min residence time. 8% solid loading and salinity 38 g/L.

therefore the monosaccharide concentrations in the hydrolysate decrease with increasing temperature, and the byproduct compounds increases. Moreover, the presence of multiple organic compounds during subcritical water hydrolysis affects the carbohydrate decomposition rate (Daneshvar et al., 2012). Previous studies on water hydrolysis of *Ulva pertusa* kjellmann showed a 7.4% (w/w) glucose conversion yield at 180 °C and 8 min of residence time (Choi et al., 2013). The difference can be partly attributed to higher initial feedstock starch concentration (20.1±2.14%, w/w in (Choi et al., 2013) vs. 4.9% in this study) and longer treatment times in our study, which lead to further glucose degradation. Similar results were obtained compared to the study in ref (Meillisa et al., 2015), with brown seaweed water hydrolysis, where 1.1% glucose yield at 180 °C, 0.9% glucose yield at 220 °C, 0.6% glucose yield at 260 °C were reported. However, the carbohydrate content of the biomass in that study was not specified.

Glucose was also the major released monosaccharide from the US biomass under the tested conditions (59% starch extraction yield, out of the potentially extractable starch content). The maximum average yield achieved was 10.4±0.46 mg glucose/g dry *Ulva* sp. (21% (w glucose/w dry starch from *Ulva*), at 179 °C, 40 min residence time (8% solid load, 100% salinity). Temperature (p-val $< 1.83 \cdot 10^{-5}$), retention time (p-val < 0.003) and their combination (p-val < 0.001) are significant in glucose release from the whole biomass. Comparing the result to a starch thermal hydrolysis study (Gagić et al., 2018) shows a similarity with 19% (w/w) glucose yield obtained at 180 °C and 40 min of residence time. In another starch thermal hydrolysis study (Rogalinski et al., 2008), glucose yield was higher (30% (w/w)) with 260 °C, 2 min residence time, and decreased sharply at a longer residence time.

Glucose was also the major released monosaccharide from cellulose extracted from UC under the tested conditions. The maximum yield achieved was 0.2±0.07 mg glucose/g dry *Ulva* sp. (2.2% w/w) glucose/dry cellulose from *Ulva*), at 259 °C, 10 min residence time (8% solid load, 100% seawater salinity). Glucose yields are strongly affected by reaction temperature (p-val < 0.03), but not by the residence time (p-val $= 8.89$) or their combination (p-val $= 0.1$). The maximum obtained glucose exhibits increasing values with lower temperatures (Fig. 1**).** The obtained glucose yield shows that cellulose decomposition to glucose takes place at a higher temperature (220–260 °C) compared to the starch (180 °C) since the hydrogen bond in cellulose is more difficult to hydrolyze than in starch. However, glucose is unstable under that temperature, and accordingly, it is degraded by following reactions such as degradation and isomerization (Rogalinski et al., 2008). It could be assumed that in the experiment conditions, with a long preheating time of the reactor, most of the glucose from cellulose decomposition undergoes degradation and isomerization reactions.

The glucose yield from hydrolysates of whole *Ulva* sp. and its extracted starch fraction separately as a feedstock at similar hydrothermal process conditions are shown in Fig. 1. It can be seen that, at similar hydrothermal process conditions (180–220 °C), most of the glucose is derived from the starch fraction. However, in the case of the cellulose fraction, the glucose released at the same process conditions is very low, Fig. 1**.** The best yield of glucose from the US (based on the yield from the whole biomass) is lower than the corresponding yield from the whole *Ulva* biomass. However, we may consider the hypothetical case where all of the starch is extracted from the *Ulva* biomass rather than only 59%, and assuming that the yield of conversion from extracted starch to glucose is the same as presented above. In this case, the hypothetical yield would be 17.7 ± 2.0 mg glucose/g dry *Ulva* sp. Adding the small contribution of separate glucose production from UC, the total hypothetical yield is 17.8 ± 2.2 mg glucose/g dry *Ulva* sp. This is slightly higher than the yield from the whole *Ulva,* but the difference is within the range of measurement uncertainty. The conclusion is then that the hydrothermal treatment of separate fractions does not lead to higher glucose production even in the hypothetical case of complete starch extraction. An additional conclusion here is that starch is the major source of glucose release from *Ulva* biomass using hydrothermal hydrolysis. As starch content in Ulva could vary from 1.59% to 21.44% depending on growth conditions and seasons (Prabhu et al., 2019b), in many cases, we can expect higher total glucose yields than that shown in this study where the initial starch content was only 5.7 ± 0.32%.

The glucose yield from the starch fraction was 212.4±16.43 mg glucose/g dry US vs 16.1±0.8 mg glucose/g dry *Ulva* sp. whole biomass. The concentration of glucose in the hydrolysate of purified starch is significantly higher, which is an advantage for cost-efficient biofuel production (Larsson and Zacchi, 1996). The direct production of a concentrated stream of glucose reduces the need for additional downstream processes for glucose concentration. These processes, such as evaporation, ion exchange, or nanofiltration, are more complex and expensive than starch granules separation at the initial biomass processing stages.

The maximum average yield achieved for rhamnose, a rare sugar derived from the deconstruction of hemicellulose was 6.2±0.45 mg rhamnose/g dry *Ulva* sp., at 177 °C, 20 min residence time. No rhamnose was detected in hydrolysates from the US or the UC. These results were expected as rhamnose is a major building block of ulvan, a water-soluble cell wall polymer of *Ulva* sp.(Kidgell et al., 2019). The maximum average yield achieved for galactose, a sugar derived from the deconstruction of hemicellulose under the tested conditions, was 1.0±0.11 mg galactose/g dry *Ulva sp.*, at 180 °C, 40 min residence time. No galactose was obtained from the starch or the cellulose that was prepared from the *Ulva*.

The maximum average yield achieved for xylose, a sugar derived from the deconstruction of hemicellulose under the tested conditions, was 1.6±0.22 mg xylose/g dry *Ulva* sp., at 177 °C, 20 min residence time. The maximum average yield achieved for xylose obtained from the US was 0.1±0.01 mg /g dry *Ulva* sp. (1.2±0.14 mg xylose /g dry US), at 179 °C, 40 min treatment time. No xylose was observed in hydrolysates from UC. The maximum average yield achieved for fructose, a sugar derived from the deconstruction of cellulose and starch under the tested conditions, was 2.8±0.41 mg fructose/g dry *Ulva* sp., at 180 °C, 40 min treatment time. The maximum average yield achieved for fructose from the US was 1.3±0.11 mg fructose/g dry *Ulva* sp. (24.2±2.17 mg fructose/g dry US), at 179 °C, 40 min treatment time. No fructose was detected from the UC.

The maximum average total sugar yield achieved from the deconstruction of whole *Ulva* sp. and its carbohydrates fractions under the tested conditions, was 27.1±1.83 mg sugar/g dry *Ulva* sp., at 180 °C, 40 min treatment time. The maximum average yield achieved for total sugar from the US was 12.8±0.58 mg sugar/g dry *Ulva* sp., at 179 °C, 40 min residence time. The maximum average yield achieved for total sugar obtained from the separated UC was 0.2 mg sugar/g dry *Ulva* sp., at 259 °C, 10 min residence time**.** Total sugar yields are strongly affected by reaction temperature (like glucose yield, which is the major released monosaccharide from *Ulva* sp.), as shown in Fig. 1**e-f.**

The total sugar yield from the two fractions US and UC is significantly lower than the yield from the whole *Ulva*. If we repeat the same estimate as above under the assumption of complete starch extraction rather than 59%, the total sugar yield will be 21.9 ± 1.9 mg sugar/g dry *Ulva* sp. This is still lower than the yield of total sugars by direct hydrothermal treatment of the *Ulva* biomass. The separation into starch and cellulose fractions then is not effective for the production of total sugars. This is explained by the presence of the additional major cell wall polysaccharide ulvan, which can constitute 9 to 36% dry weight of the biomass of *Ulva* and is mainly composed of sulfated rhamnose, xylose, and uronic acids (glucuronic acid and iduronic acid) (Kidgell et al., 2019).

3.5. The PHA production yield from seaweed hydrolysate

The whole seaweed (*Ulva* sp.) or its fraction (US and UC) hydrolysates were used for PHA production by *Haloferax mediterranei*. The maximum PHA yield was observed with *Ulva* sp. hydrolysate at 180 °C, 40 min treatment time, (Table 1**,** Fig. 1**a**): 1 g of dry *Ulva* sp. yielded

Table 1
Summary of highest glucose, PHA, and hydrochar yields produced from the different biomass hydrolysis based on the highest glucose yields. All cases are with solid loading 8% and 100% water salinity (38 g/L sea salts).

Raw material	Process conditions	Glucose| (mg/g dry *Ulva* sp.)	PHA (mg/g dry *Ulva* sp.)	Hydrochar (g/g dry *Ulva* sp.)	Exp #
Seaweed biomass *(*whole *Ulva* sp.*)*	180 °C 40 min	16.1 ± 0.47	77.8 ± 0.66	0.186 ± 0.042	3, 6
Extracted starch from *Ulva* sp.	180 °C 40 min	11.2 ± 0.61	5.1 ± 0.02	0.106 ± 0.056	21, 24
Extracted cellulose from *Ulva* sp.	260 °C 10 min	0.2 ± 0.06	3.5 ± 0.12	0.411 ± 0.294	49, 52

77.8 ± 0.66 mg of PHA. For the starch fraction from *Ulva* sp., the maximum PHA yield was observed at 180 °C, 40 min treatment time, (Table 1): 1 g of dry *Ulva* sp. yielded approximately 5.1 ± 0.02 mg of PHA. For the cellulose fraction, the maximum PHA yield was observed at 260 °C and 10 min treatment time (Table 1): 1 g of *dry Ulva* sp. yielded approximately 3.5 ± 0.12 mg of PHA. Consequently, a maximum PHA production can be achieved when the whole seaweed is hydrothermally processed. Whole seaweed hydrolysate is much richer media for archaea growth than starch or cellulose hydrolysates alone as it releases components such as amino acids, fatty acids, and various micronutrients coming from the seaweed, the absence of which could limit the growth even in carbon-rich media. Previous studies on PHA production from seaweed biomass have reported yields ranging from 10 to 120 mg g^{-1} of macroalgal biomass. For example, Ghosh et al., 2019 reported a maximum PHA yield of 110 mg g^{-1} *Ulva* utilizing macroalgal biomass hydrolysates as a substrate (Ghosh et al., 2019). Tuma et al., 2020 reported a maximum PHA yield of 43 mg g^{-1} of *Gelidium* biomass (Tůma et al., 2020). Bera et al., 2015 used seaweed derived crude levulinic acid as a substrate and obtained a yield of 95 mg g^{-1} of *Kappaphycus* biomass (Bera et al., 2015). Another study by Azizi et al., 2017 reported a PHA yield of 14.8 mg g^{-1} of *Sargassum* using brown seaweed as a substrate (Azizi et al., 2017). Similar studies by Alkotaini et al., 2016 yielded a PHB yield of 54 mg g^{-1} of *Gelidium amansii* biomass using *B. megaterium* as the fermentative organism (Alkotaini et al., 2016). Sawant et al., 2018 reported a maximum PHA yield of 31.2 mg g^{-1} of *Gelidium amansii* biomass in a 2L controlled batch fermenter (Sawant et al., 2018). Further optimizations of cultivation conditions (pH, temperature, salinity, inoculum strength, and C / N ratio) are required for enhancement of PHA production using macroalgal hydrolysate as substrate.

3.6. Properties of Ulva starch, cellulose, and their hydrochars

The untreated *Ulva* sp. biomass and its hydrochar obtained in the experiment with the highest total monosaccharides yield were analyzed, and the ultimate, proximate, and HHV are summarized in Table 2. The hydrochar carbon content increased and oxygen content decreased compared to the untreated biomass due to the carbonization process, thus upgrading the HHV by 8.9 MJ/kg, from 12.3 to 21.2 MJ/kg, (energy densification of 1.7–1.8) compared to the initial sample. The energy gain ratio (energy densification multiplied by hydrochar yield) is 0.31–0.34, slightly lower than other studies on seaweed which show a 0.39–0.67 energy gain ratio of (Daneshvar et al., 2012; Smith and Ross, 2016; Xu et al., 2013). A previous study on hydrothermal carbonization of three kelps *Laminaria digitata, Laminaria hyperborea,* and *Alaria esculenta* at 250 °C, shows increasing of the caloric value from 11.4 to 22.6 MJ/kg, 11.2 to 24.1 MJ/kg, and 12.8 to 24.7 MJ/kg, respectively (Smith and Ross, 2016).

The proximate, ultimate, and HHV analysis of the US and the US hydrochar are shown in Table 2**.** The US hydrochar carbon content increased, and oxygen content decreased compared to the original biomass due to the carbonization process, similar to the changes reported in the HTC study on corn starch (Malumba et al., 2009). The HHV increased from 12.3 to 19.1 MJ/kg (energy densification of 1.6) compared to the initial *Ulva* DW sample. The energy recovery ratio relative to original biomass DW (energy densification multiplied by hydrochar yield) is 0.15.

The proximate, ultimate, and HHV analysis of the untreated UC and its UC hydrochar are shown in Table 2. The carbon content of the hydrochar obtained from the UC increased compared to the untreated biomass, due to the carbonization process. Thus, the results could indicate dehydration and decarboxylation reactions scheme (Toor et al., 2011). It can be seen that the HTC process increased the hydrochar HHV by 9.8 MJ/kg, from 12.3 to 22.1 MJ/kg, compared to the initial untreated *Ulva* DW sample, a 0.40 energy recovery gain. Similarly to other HTC studies on cellulose, which show a 0.39–0.67 energy recovery ratio of (Daneshvar et al., 2012; Smith and Ross, 2016; Xu et al., 2013).

Scanning electron microscopy morphology of the *Ulva* sp. biomass and the *Ulva* sp. hydrochar shows that in the experiment conditions (180 °C and 40 min treatment time) the highly organized porous structures were disrupted. Similar behavior is presented in previous SEM reports on seaweed hydrochar production (Sun et al., 2016).

In the SEM morphology of the UC and UC hydrochar, agglomerated

Table 2
Ulva sp. biomass, Ulva starch (US), Ulva cellulose (UC) and hydrochar properties. Hydrochar produced at 180 °C, Solid Loading 8%, 40 min, salinity 38 g/L.

		Ulva sp. Untreated	*Ulva* sp. hydrochar	US untreated	US hydrochar	UC Untreated	UC hydrochar
Ultimate (wt. %)	N (%)	1.46 ± 0.01	3.0 ± 0.73	1.14 ± 0.06	1.63 ± 0.11	0.67 ± 0.03	0.51 ± 0.02
	C (%)	24.77 ± 0.13	44.4 ± 0.8	38.45 ± 0.16	52.37 ± 0.81	40.81 ± 0.62	56.59 ± 0.76
	H (%)	4.88 ± 0.02	5.8 ± 0.0	6.34 ± 0.08	3.82 ± 0.11	6.21 ± 0.04	4.88 ± 0.26
	S (%)	6.64 ± 0.1	3.1 ± 0.5	0.62 ± 0.12	0.61 ± 0.1	0.11 ± 0.05	0.0 ± 0.00
	O (%)	34.41 ± 0.26	26.3 ± 1.15	50.02 ± 2.06	38.09 ± 1.04	52.21 ± 1.32	34.47 ± 0.95
Proximate (dry wt. %)	Ash	27.85 ± 0.51	17.35 ± 0.15	3.44 ± 0.26	1.97 ± 0.08		3.14 ± 0.18
	Moisture	18.12 ± 1.31	13.76 ± 0.3	5.26 ± 0.22	14.66 ± 0.40		8.04 ± 0.19
Biochemical (wt. %)	Starch	6.83 ± 0.07					
	Cellulose	7.76 ± 0.14					
	Ulvan*	13.88 ± 0.40%					
	Protein**	7.31 ± 0.05					
	Lipids*	3.81 ± 0.04					
HHV (MJ kg-1)	(Boie, 1953)	11.2	20.4	15.4	18.9	1.3	21.7
	(Grummel and Davies, 1933)	9.5	17.9	12.8	16.5	4.9	19.2
	Measured value (Calorimeter)	12.1 ± 0.2	20.4 ± 0.8	14.34 ± 1.16	19.1 ± 1.25	16.07 ± 0.62	22.14 ± 1.56

* Lipids and ulvan were measure in our previous work in (Prabhu et al., 2020) **Protein content was calculated by the conversion factor of 5 from total nitrogen content.

micro spherical granules with the fragmented surface are visible. The US starch hydrochar has similar morphology and typical particle size to those synthesized by HTC treatment of corn starch (Reza et al., 2014). The SEM morphology of UC and UC hydrochar show that part of the cellulose structure was disintegrated, and the overall morphology is not homogeneous. Particle structures show a similarity to the previous study on cellulose hydrochar (Wang et al., 2018).

The ash-free solid residue comprising hydrochar and water-soluble compounds are shown in Fig. 2**b** and Table 2, 3. As the %salinity of the experiments is known (3.8%) and the %ash of the biomass was measured, the total ash-free solids (AFS) can be calculated (as can be seen **Eq.1**). During the residue extraction, some losses occur (e.g., solids sampling line, solids attached to the stirrer, etc.), and the total ash-free solid recovery is 83–88% of the initial ash-free biomass. The hydrochar yields vary in the range of 5–51%, with the highest value at 180 °C and decreased at a higher temperature (220–260 °C). These changes in biochar recovery show similarity to other HTC studies, as reported in (Smith and Ross, 2016; Wang et al., 2018; Xu et al., 2013). The hydrochar mass recovery from starch fraction shows a resemblance to solid recovery from corn starch at 180 °C as reported by Zhao et al.(Zhao et al., 2016) The hydrochar mass recovery from the cellulose fraction shows a sharp decrease at higher temperatures (220–260 °C). Similar behavior of the cellulose derived from hydrothermal carbonization at 220–260 °C is reported in(Hoekman et al., 2013). The rest of the mass can be attributed to the release of moisture, water formation during the carbonization process, and volatile molecules.

Table 3
Solid ash-free mass recovery.

Exp #	Hydrochar yield (w/w) *	Water-soluble solid yield (w/w) *	Total solid yield (w/w) *
3	18.8%	65.4%	84.2%
6	18.3%	67.3%	85.6%
9	16.9%	68.8%	85.6%
12	15.5%	72.3%	87.8%
15	13.2%	73.2%	86.4%
18	12.6%	74.1%	86.7%
21	10.6%	72.1%	82.7%
24	11.5%	73.2%	84.6%
27	9.1%	74.2%	83.3%
30	8.3%	76.4%	84.7%
33	5.3%	80.4%	85.7%
36	4.8%	77.3%	82.1%
39	51.1%	34.8%	85.9%
42	48.2%	38.1%	86.2%
45	38.9%	44.7%	83.6%
48	43.1%	42.0%	85.1%
51	29.5%	56.9%	86.3%
54	25.4%	61.5%	86.9%

* Ash-free mass recovered from initial ash-free dry biomass.

The solid residue was characterized in the case where the experimental conditions lead to the highest total monosaccharide yield. It was found that at 180 °C, residence time 40 min solid loading of 8% and water salinity of 38 g/L, the hydrochar ash-free solids (AFS) yields (w/

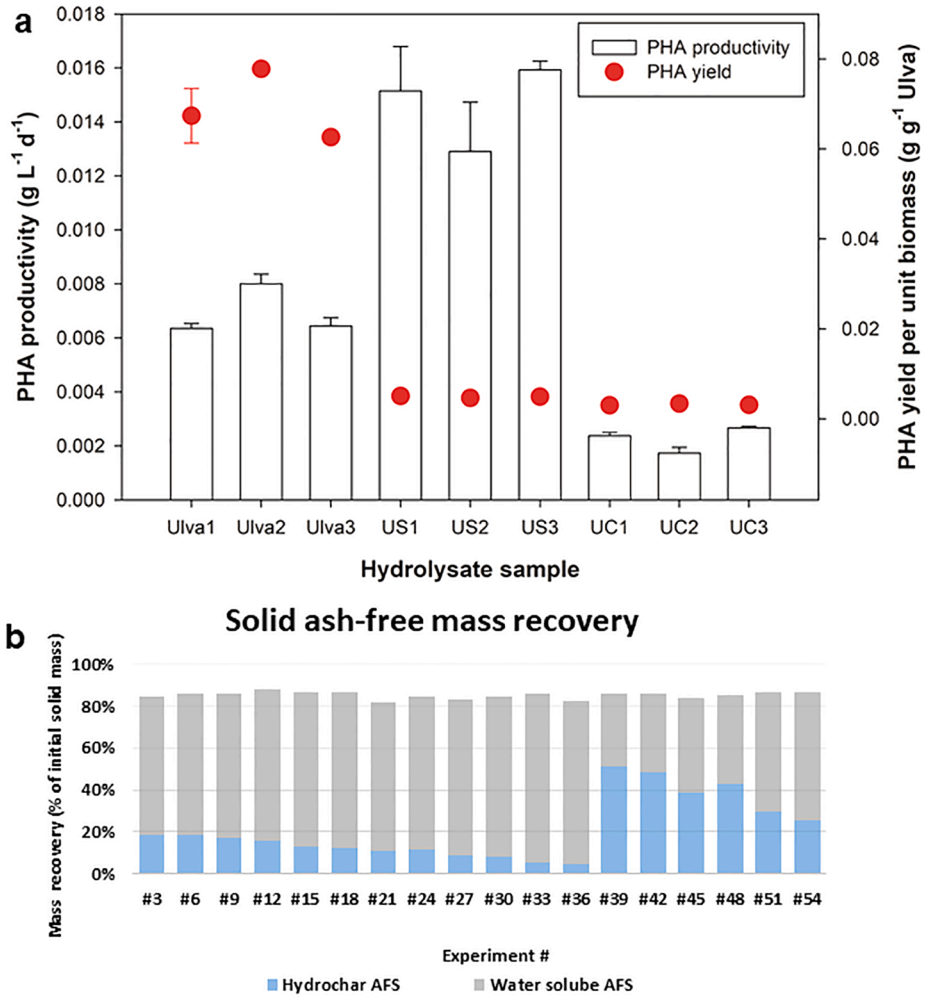

Fig. 2. a. PHA productivity from hydrolysates fermented with *Haloferax mediterranei* b. Mass balance summary for organic compounds from the hydrothermally treated biomass.

w) of the whole seaweed and its starch and cellulose fractions, were 18.6 ± 0.42%, 10.6 ± 0.56%, and 41.1 ± 2.94% respectively (Table 3). Additionally, it has been observed that UC and US hydrochar have much less ash and higher carbon content than whole *Ulva* hydrochar (Table 2). This means that ash, composed of inorganic matter, moves from the biomass to the hydrolysate and will require further treatment in the water fraction.

3.7. Cost-benefit analysis

In this section, we denote the hydrolysis of the whole *Ulva* sp. as case *A* and the extraction of starch and cellulose as case *B*. Both production processes can be represented by a fixed proportion (Leontief) technology that links inputs (especially *Ulva* sp.) and outputs (i.e., three main ones: glucose, PHA, and hydrochar). The gross margin, i.e., profits without fixed cost (π_A) of process *A* can be written as

$$\pi_A = P_G Q_G^A + P_{PHA} Q_{PHA}^A + P_H Q_H^A - \left(P_{SW} + c_0^A\right) Q_{SW}^A \quad (7)$$

where P_G, P_{PHA}, P_H, and P_{SW}denote market prices of glucose, PHA, hydrochar, and seaweed; c_0^A is the processing cost of one metric ton of dry seaweed; and Q_G^A, Q_{PHA}^A, and Q_H^A are quantities (in metric tons) of outputs corresponding to the quantity of seaweed Q_{SW}^A (also measured in metric tons). It should be noted that because the focus of our economic analysis is on the three main outputs, we account for costs of other inputs (e.g., electricity or ethanol for bleaching) and the benefits of all other possible outputs in the term c_0^A. It should, therefore, be interpreted as the net operating cost other than the cost of the main feedstock. The gross margin for process *B* is calculated similarly. If we knew the future production capacity of a commercial seaweed processing plant and the expected payback period of the project, we could estimate the capital (fixed) cost per metric ton of seaweed. This would then be added to the term c_0^Ain **Eq. (7)**.

A property of a fixed-proportion technology is that if inputs are scaled by a certain factor, outputs change accordingly. This is convenient in our case, as we can assume without loss of generality that the amount of seaweed used in both processes is one metric ton and then use the values from Table 2 to determine that $Q_G^A = 16.1$ kg, $Q_{PHA}^A = 77.8$ kg, and $Q_H^A = 186$ kg (we take the mean values reported in Table 2 for our baseline). For production process *B*, we add the respective values in Table 2 as we are interested in the total production of individual outputs; thus, we obtain: $Q_G^B = 11.4$ kg, $Q_{PHA}^B = 8.6$ kg, and $Q_H^B = 517$ kg.

The production cost of seaweed varies, depending on the type, location of production, and production system used. We use the Food and Agriculture Organization of the United Nations (FAO) trade data (FAO, 2018)(FAO, 2018) to estimate the price of seaweed per metric ton of dry weight (DW). In 2016, the EU imported 88,485 tons of non-edible seaweed at the total value of 69.5 million US dollars; this gives an average price of 785 US dollars per ton; therefore, we set $P_{SW} = 700$ euros per ton (0.70 euros per kilogram).

We assume the produced glucose will be used industrially to produce ethanol. We, therefore, proxy its price with the price of sugar and set it equal to $P_G = 0.36$ euros per kilogram, which corresponds to the average price in 2016 (Https://www.indexmundi.com/commodities/?commodity=sugar&months=60&currency=eur, n.d.). The price of PHA varies between 4 euros and 10 euros per kilogram, depending on use (Bugnicourt et al., 2014; Kourmentza et al., 2017); we take the middle value for our baseline and assume $P_{PHA} = 7$ euros per kilogram.

Hydrochar can be burned along with coal or used as fertilizer, among other uses. To be on the conservative side, we assume most of it will be burned. We, therefore, assume$P_H = 0.06$ euros per kilogram, which is in line with the price of coal (Https://www.indexmundi.com/commodities/?commodity=coal-australian&months=120&currency=eur, n.d.).

Given the prices and quantities of individual outputs, we can evaluate their economic importance in generating the total revenue based on equation (7) (i.e., the receipts from sales of glucose, PHA, and hydrochar). Fig. 3**a** depicts the situation for case *A* (processing the whole *Ulva* sp.) and Fig. 3**b** for case *B* (separation of starch and cellulose). In both cases, PHA takes the lion's share of revenues, suggesting it is the most economically important output of both production processes (given the baseline output prices).

Another important piece of information for the economics of both production processes is under what circumstances would the production process be profitable (i.e., the gross margin would be positive) and which production process would economically be preferable. Because we do not know the actual processing costs c_0^A and c_0^B, we can estimate their threshold values by omitting the fixed cost (as we do not know it) and setting the gross margins to zero (i.e., the breakeven point). After rearranging the equations for zero gross margins, we obtain

$$\overline{c}_0^A = \frac{P_G Q_G^A + P_{PHA} Q_{PHA}^A + P_H Q_H^A}{Q_{SW}^A} - P_{SW} \quad (8)$$

$$\overline{c}_0^B = \frac{P_G Q_G^B + P_{PHA} Q_{PHA}^B + P_H Q_H^B}{Q_{SW}^B} - P_{SW} \quad (9)$$

The thresholds estimated by equations (8) and (9) provide only rough indications for the economics of the production processes because the fixed capital cost of starting the production might be high. As mentioned earlier, the capital (fixed) cost per unit metric ton of seaweed will depend on the planned production capacity and the expected payback period of the investment. This means that the actual thresholds of the processing cost will be higher than our estimates.

Setting $Q_{SW}^A = Q_{SW}^B = 1$ kg and using the prices and corresponding quantities from above, we obtain$\overline{c}_0^A = -0.14$ euros per kilogram and $\overline{c}_0^B = -0.60$ euros per kilogram. These values provide us with two important pieces of information. First, neither production process is economically feasible for the given constellation of production parameters (i.e., yields are small relative to inputs) and prices (the market prices of outputs would need to be higher or the price of seaweed lower). Second, a lower (absolute) value of the breakeven cost of process *A* suggests that this process is closer to economic feasibility (provided the revenues can at least cover the cost).

3.8. Economics sensitivity analysis

The results in the previous section show that for the baseline vector of input and output prices, neither of the production processes would pay off economically. In this section, we will perform sensitivity analysis concerning i) the price of seaweed and ii) production parameters to determine the breakeven points. The lack of precise information on the processing costs (c_0^A and c_0^B) of seaweed for the two processes above allows us to answer only two specific questions: i) what is the maximum price of seaweed and ii) what are the necessary amounts of outputs, such that either production process yields a zero gross margin assuming the processing cost is zero? To do so, we set the right-hand side of **Eq. (8)** and **Eq. (9)** to zero and solve the resulting equation for the unknown values (holding other prices/parameters at their baseline values).

For production process *A*, the price of *Ulva* sp would have to be 561 euros per metric ton of dry weight (80% of the baseline price) for revenues to just cover the cost of feedstock, assuming the processing cost is zero. For production process *B*, the threshold price of *Ulva* sp is 95 euros per metric ton of dry weight (14% of baseline). These results illustrate that the latter process is less likely to be economically feasible, given the very low required price of *Ulva* sp. These results should also be interpreted carefully. Suppose the price of *Ulva* is 300 euros per metric ton of DW. Does it automatically mean that production process *A*, for example, yields a positive gross margin? The answer is negative. Using **Eq. (8)**, we calculate the maximum processing cost for the process to breakeven economically to be $c_0^A = 262$ euros per metric ton of DW. Only if the actual processing cost were below this value, the gross margin would be positive (and this would still ignore the fixed cost). For process *B*, when

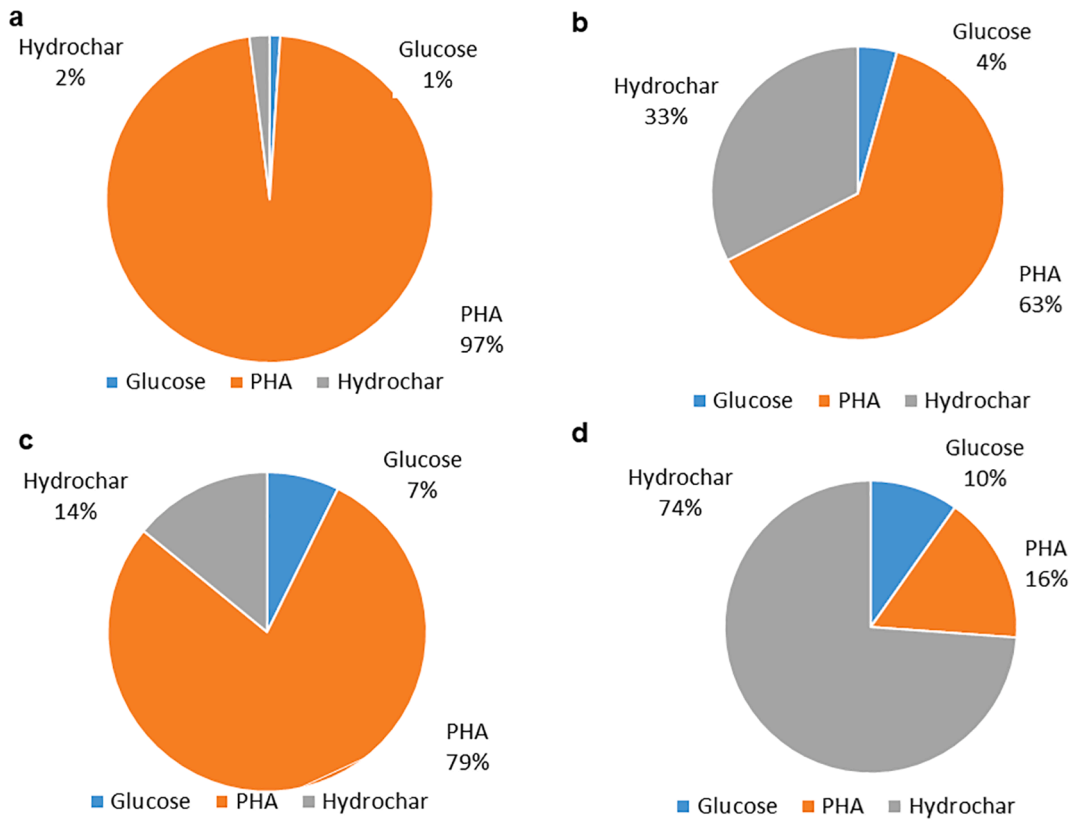

Fig. 3. The relative importance of individual products in total revenues a. case *A* (whole *Ulva sp*.). b. case *B* (extraction of Ulva starch and Ulva cellulose).

the price of *Ulva* sp is 300 euros per metric ton of DW, $c_0^B = -205$ euros per metric ton of DW, meaning that the feedstock price is still too high for this process to breakeven.

Table 4 presents the results of the sensitivity analysis concerning the production parameters of both processes (prices are the same as in the baseline). The key question this table answer is: how much do we need to change individual production parameters (in bold) compared to the baseline (the first line for either process) for the revenues to be equal to the cost of Ulva. In both cases, we first change one parameter at a time (although it might not be realistic technically) and then prorate all parameters by the same factor. Overall, the results indicate that both production processes would need to generate significantly more outputs from one unit of input. Increasing the leading product (PHA) is the only feasible option for A. The other products make negligible contributions, and the required increase in them will never be practical.

Because the baseline price of PHA of 7 euros per kilogram is not competitive with the price of plastics, we would like to know how the results in Table 4 would change if the price of PHA were on the par with the price of polyester fiber (PHA as a substitute for plastic). At the time of writing, polyester sells at a price in the region of 590 to 1000 euros per metric ton. We take the value of 800 euros per metric ton (0.8 euros per kilogram) for our sensitivity analysis.

Fig. 3**c** depicts the situation for case *A* (processing the whole *Ulva* sp.) and Fig. 3**d** for case *B* (separation of starch and cellulose) for the low PHA prices. Unlike in the high PHA price scenario, hydrochar became the most significant contributor to the economics of the system of case *B*. In case *A*, PHA still takes the major share of revenues.

Results of a sensitivity analysis of a change in the price of PHA on the

Table 4
Theoretical percentage changes of the baseline production parameters needed for both processes to breakeven economically at zero processing cost.

	Glucose	PHA	Hydrochar
Process A (whole Ulva)			
Baseline (g/g)	0.0161	0.0778	0.186
% change only glucose	**2389**	0	0
% change only PHA	0	**25**	0
% change only hydrochar	0	0	**1241** †
% change all	**25** †	**25** †	**25** †
Process B (extraction first)			
Baseline (g/g)	0.0114	0.0086	0.517
% change only glucose	**14,734** †	0	0
% change only PHA	0	**1004**	0
% change only hydrochar	0	0	**1949** †
% change all	**634** †	**634** †	**634** †

Note: All cases are normalized to unit input. Prices of input and outputs areas in the baseline.

† The process cannot economically breakeven under any conversion yield with the current pricing on products.

Table 5
Sensitivity analysis of both production processes (under zero profits) concerning the price of PHA in comparison to fossil-derived polyesters fibers.

	Glucose	PHA	Hydrochar
Process A (whole Ulva)			
Baseline (g/g)	0.0161	0.0778	0.186
% change only glucose	**10,711** †	0	0
% change only PHA	0	**997**	0
% change only hydrochar	0	0	**5563** †
% change all	**784** †	**784** †	**784** †
Process B (extraction first)			
Baseline (g/g)	0.0114	0.0086	0.517
% change only glucose	**16,033** †	0	0
% change only PHA	0	**9564**	0
% change only hydrochar	0	0	**2121** †
% change all	**1567** †	**1567** †	**1567** †

Note: All cases are normalized to unit input. $P_{PHA} = 0.80$ euro per kilogram, all other prices as in the baseline.

† The process cannot economically breakeven under any conversion yield with the current pricing on products.

breakeven production parameters are presented in Table 5.

The results show that amount of output would have to increase significantly in all scenarios when the price of PHA decreases. This makes intuitive sense: as a lower output price worsens the economics of either production process, increased production efficiency is required to compensate for it. The key finding here is that major effort is needed to increase the conversion yield of Ulva biomass to PHA. The possible direction to address this issue could be using Ulva biomass with higher initial starch content. In the previous work, we showed that Ulva can accumulate starch up to 21.44% of DW (vs 5.7 ± 0.32% in this study), depending on the season and cultivation conditions (Prabhu et al., 2019a). In addition, while in this work we achieved 53.3% content of intracellular PHA, previous studies showed that after optimization of the cultivation condition, the intracellular content of PHA of *H. mediterranei* in can reach 75.4% (Hermann-Krauss et al., 2013). Another conclusion is that separation of glucose is not beneficial with the HTC process that we present. Not separating glucose would save fixed and operating costs. The separation of char makes a significant contribution only in the case of B under low PHA prices (Fig. 3**d**). However, B is even further from technical and economic feasibility. This indicates that also the production of hydrochar can be eliminated at higher PHA prices.

4. Conclusions

Glucose is a major released monosaccharide from *Ulva* sp. Separation of starch could be a better way for the production of glucose. Separation of cellulose could a better way to get higher hydrochar yield with lower ash content. The maximum PHA yield produced by *Haloferax mediterranei* was observed with whole *Ulva* sp. hydrolysate, indicating that separation makes the production of PHA unattractive. Economic analysis shows the advantage of direct Ulva biomass processing to PHA. The key finding is that major effort is needed to increase the Ulva biomass to PHA conversion yield for PHA to compete with fossils derived polyesters.

CRediT authorship contribution statement

Efraim Steinbruch: Investigation, Methodology, Writing - original draft. **Dusan Drabik:** . **Michael Epstein:** Investigation, Data curation, Formal analysis, Writing - review & editing. **Supratim Ghosh:** Investigation, Writing - review & editing. **Meghanath S. Prabhu:** Investigation, Writing - review & editing. **Michael Gozin:** Investigation, Writing - review & editing. **Abraham Kribus:** Investigation, Writing - review & editing. **Alexander Golberg:** Conceptualization, Methodology, Writing - original draft.

Declaration of Competing Interest

The authors declare that they have no known competing financial interests or personal relationships that could have appeared to influence the work reported in this paper.

Acknowledgments

The authors thank the Israeli Ministry of Energy, Infrastructures and Water Resources (219-11-138), TAU XIN Center, and The Aaron Frenkel Air Pollution Initiative at Tel Aviv University for the support of this study. The authors sincerely thank Vered Holdengreber from the Electron Microscopy Unit, Inter-Departmental Research Facility Unit, Faculty of Life Sciences, Tel Aviv University for the help with SEM. Dusan Drabik acknowledges the financial support received from the Slovak Research and Development Agency under contract No. APVV-19-0544 and from the Operational program Integrated Infrastructure within the project: Demand-driven research for the sustainable and innovative food, Drive4SIFood 313011V336, co-financed by the European Regional Development Fund.

Appendix A. Supplementary data

Supplementary data to this article can be found online at https://doi.org/10.1016/j.biortech.2020.124263.

References

Alkotaini, B., Koo, H., Kim, B.S., 2016. Production of polyhydroxyalkanoates by batch and fed-batch cultivations of Bacillus megaterium from acid-treated red algae. Korean J. Chem. Eng. 33, 1669–1673. https://doi.org/10.1007/s11814-015-0293-6.

Azizi, N., Najafpour, G., Younesi, H., 2017. Acid pretreatment and enzymatic saccharification of brown seaweed for polyhydroxybutyrate (PHB) production using Cupriavidus necator. Int. J. Biol. Macromol. 101, 1029–1040. https://doi.org/10.1016/j.ijbiomac.2017.03.184.

Bera, A., Dubey, S., Bhayani, K., Mondal, D., Mishra, S., Ghosh, P.K., 2015. Microbial synthesis of polyhydroxyalkanoate using seaweed-derived crude levulinic acid as co-nutrient. Int. J. Biol. Macromol. 72, 487–494. https://doi.org/10.1016/j.ijbiomac.2014.08.037.

Boie, W., 1953. Fuel Technology Calculations. Energietechnik 3.

Bugnicourt, E., Cinelli, P., Lazzeri, A., Alvarez, V., 2014. Polyhydroxyalkanoate (PHA): Review of synthesis, characteristics, processing and potential applications in packaging. Express Polym. Lett. https://doi.org/10.3144/expresspolymlett.2014.82.

Chien, C.C., Ho, L.Y., 2008. Polyhydroxyalkanoates production from carbohydrates by a genetic recombinant Aeromonas sp. Appl. Microbiol. Lett. https://doi.org/10.1111/j.1472-765X.2008.02471.x.

Choi, W.-Y.-Y., Kang, D.-H.-H., Lee, H.-Y.-Y., 2013. Enhancement of the saccharification yields of Ulva pertusa kjellmann and rape stems by the high-pressure steam pretreatment process. Biotechnol. Bioprocess Eng. 18, 728–735. https://doi.org/10.1007/s12257-013-0033-x.

Daneshvar, S., Salak, F., Ishii, T., Otsuka, K., 2012. Application of subcritical water for conversion of macroalgae to value-added materials. Ind. Eng. Chem. Res. 51, 77–84. https://doi.org/10.1021/ie201743x.

El-Sayed, W.M.M., Ibrahim, H.A.H., Abdul-Raouf, U.M., El-Nagar, M.M., 2016. Evaluation of Bioethanol Production from Ulva lactuca By Saccharomyces cerevisiae. J Biotechnol Biomater 6. https://doi.org/10.4172/2155-952X.1000226.

FAO, 2018. The global status of seaweed production, trade and utilization.

Gagić, T., Perva-Uzunalić, A., Knez, Ž., Škerget, M., 2018. Hydrothermal Degradation of Cellulose at Temperature from 200 to 300 °c. Ind. Eng. Chem. Res. https://doi.org/10.1021/acs.iecr.8b00332.

Ghosh, S., Gnaim, R., Greiserman, S., Fadeev, L., Gozin, M., Golberg, A., 2019. Macroalgal biomass subcritical hydrolysates for the production of polyhydroxyalkanoate (PHA) by Haloferax mediterranei. Bioresour. Technol. https://doi.org/10.1016/j.biortech.2018.09.108.

Greiserman, S., Epstein, M., Chemodanov, A., Steinbruch, E., Prabhu, M., Guttman, L., Jinjikhashvily, G., Shamis, O., Gozin, M., Kribus, A., Golberg, A., 2019. Co-production of Monosaccharides and Hydrochar from Green Macroalgae Ulva (Chlorophyta) sp. with Subcritical Hydrolysis and Carbonization. BioEnergy Res. 1–14 https://doi.org/10.1007/s12155-019-10034-5.

Grummel, E.S., Davies, I., 1933. A new method of calculating the calorific value of a fuel from its ultimate analysis. Fuel 12, 199–203.

Hargreaves, P.I., Barcelos, C.A., da Costa, A.C.A., Pereira Jr, N., Pereira, N., Pereira Jr, N., 2013. Production of ethanol 3G from Kappaphycus alvarezii: evaluation of different process strategies. Bioresour. Technol. 134, 257–263. https://doi.org/10.1016/j.biortech.2013.02.002.

Hermann-Krauss, C., Koller, M., Muhr, A., Fasl, H., Stelzer, F., Braunegg, G., 2013. Archaeal production of polyhydroxyalkanoate (PHA) Co- and terpolyesters from biodiesel industry-derived by-products. Archaea 2013. https://doi.org/10.1155/2013/129268.

Hoekman, S.K., Broch, A., Robbins, C., 2011. Hydrothermal Carbonization (HTC) of Lignocellulosic Biomass. Energy & Fuels 25, 1802–1810. https://doi.org/10.1021/ef101745n.

Hoekman, S.K., Broch, A., Robbins, C., Zielinska, B., Felix, L., 2013. Hydrothermal carbonization (HTC) of selected woody and herbaceous biomass feedstocks. Biomass Convers. Biorefinery 3, 113–126. https://doi.org/10.1007/s13399-012-0066-y.

Https://www.indexmundi.com/commodities/?commodity=coal-australian&months=120&currency=eur, n.d. Coal Monthly price.

Https://www.indexmundi.com/commodities/?commodity=sugar&months=60&currency=eur, n.d. Sugar Monthly Price - Euro per Kilogram.

Jiang, R., Linzon, Y., Vitkin, E., Yakhini, Z., Chudnovsky, A., Golberg, A., 2016. Thermochemical hydrolysis of macroalgae Ulva for biorefinery: Taguchi robust design method. Sci. Rep. 6.

Kahar, P., Tsuge, T., Taguchi, K., Doi, Y., 2004. High yield production of polyhydroxyalkanoates from soybean oil by Ralstonia eutropha and its recombinant strain. Polym. Degrad. Stab. https://doi.org/10.1016/S0141-3910(03)00227-1.

KANTARLI, İ.C., PALA, M., YILDIRIM, Y., YANIK, J., ABREU, M.H., 2019. Fuel characteristics and combustion behavior of seaweed-derived hydrochars. TURKISH J. Chem. https://doi.org/10.3906/kim-1807-7.

Khambhaty, Y., Mody, K., Gandhi, M.R., Thampy, S., Maiti, P., Brahmbhatt, H., Eswaran, K., Ghosh, P.K., 2012. Kappaphycus alvarezii as a source of bioethanol. Bioresour. Technol. 103, 180–185. https://doi.org/10.1016/j.biortech.2011.10.015.

Kidgell, J.T., Magnusson, M., de Nys, R., Glasson, C.R.K., 2019. Ulvan: A systematic review of extraction, composition and function. Algal Res. https://doi.org/10.1016/j.algal.2019.101422.

Klein-Marcuschamer, D., Oleskowicz-Popiel, P., Simmons, B.A., Blanch, H.W., 2012. The challenge of enzyme cost in the production of lignocellulosic biofuels. Biotechnol. Bioeng. 109, 1083–1087. https://doi.org/10.1002/bit.24370.

Korzen, L., Peled, Y., Shamir, S.Z., Shechter, M., Gedanken, A., Abelson, A., Israel, A., 2015. An economic analysis of bioethanol production from the marine macroalga Ulva (Chlorophyta). TECHNOLOGY 03, 114–118. https://doi.org/10.1142/S2339547815400105.

Kourmentza, C., Plácido, J., Venetsaneas, N., Burniol-Figols, A., Varrone, C., Gavala, H. N., Reis, M.A.M., 2017. Recent Advances and Challenges towards Sustainable Polyhydroxyalkanoate (PHA) Production. Bioengineering 4, 55. https://doi.org/10.3390/bioengineering4020055.

Larsson, M., Zacchi, G., 1996. Production of ethanol from dilute glucose solutions. A technical- economic evaluation of various refining alternatives. Bioprocess Eng. https://doi.org/10.1007/BF00369615.

Le Corre, D., Bras, J., Dufresne, A., 2010. Starch nanoparticles: A review. Biomacromolecules. https://doi.org/10.1021/bm901428y.

Malumba, P., Doran, L., Zanmenou, W., Odjo, S., Katanga, J., Blecker, C., Béra, F., 2017. Morphological, structural and functional properties of starch granules extracted from the tubers and seeds of Sphenostylis stenocarpa. Carbohydr. Polym. 178, 286–294. https://doi.org/10.1016/j.carbpol.2017.09.013.

Malumba, P., Massaux, C., Deroanne, C., Masimango, T., Béra, F., 2009. Influence of drying temperature on functional properties of wet-milled starch granules. Carbohydr. Polym. https://doi.org/10.1016/j.carbpol.2008.07.027.

Meillisa, A., Woo, H.-C.-C., Chun, B.-S.-S., 2015. Production of monosaccharides and bioactive compounds derived from marine polysaccharides using subcritical water hydrolysis. Food Chem. 171, 70–77. https://doi.org/10.1016/j.foodchem.2014.08.097.

Möller, M., Nilges, P., Harnisch, F., Schröder, U., 2011. Subcritical water as reaction environment: Fundamentals of hydrothermal biomass transformation. ChemSusChem. https://doi.org/10.1002/cssc.201000341.

Prabhu, M., Chemodanov, A., Gottlieb, R., Kazir, M., Nahor, O., Gozin, M., Israel, A., Livney, Y.D., Golberg, A., 2019a. Starch from the sea: The green macroalga Ulva ohnoi as a potential source for sustainable starch production in the marine biorefinery. Algal Res. 37, 215–227. https://doi.org/10.1016/J.ALGAL.2018.11.007.

Prabhu, M., Chemodanov, A., Gottlieb, R., Kazir, M., Nahor, O., Gozin, M., Israel, A., Livney, Y.D., Golberg, A., 2019b. Starch from the sea: the green macroalga Ulva sp. as a potential source for sustainable starch production from the sea in marine biorefineries. Algal Res. 37, 215–227. https://doi.org/10.1016/j.algal.2018.11.007.

Prabhu, M.S., Israel, A., Palatnik, R.R., Zilberman, D., Golberg, A., 2020. Integrated biorefinery process for sustainable fractionation of Ulva ohnoi (Chlorophyta): process optimization and revenue analysis. J. Appl. Phycol. https://doi.org/10.1007/s10811-020-02044-0.

Reza, M.T., Andert, J., Wirth, B., Busch, D., Pielert, J., Lynam, J.G., Mumme, J., 2014. Hydrothermal Carbonization of Biomass for Energy and Crop Production. Appl. Bioenergy 1. https://doi.org/10.2478/apbi-2014-0001.

Rodrigues, D., Freitas, A.C., Pereira, L., Rocha-Santos, T.A.P., Vasconcelos, M.W., Roriz, M., Rodríguez-Alcalá, L.M., Gomes, A.M.P., Duarte, A.C., 2015. Chemical composition of red, brown and green macroalgae from Buarcos bay in Central West Coast of Portugal. Food Chem. 183, 197–207. https://doi.org/10.1016/j.foodchem.2015.03.057.

Rogalinski, T., Liu, K., Albrecht, T., Brunner, G., 2008. Hydrolysis kinetics of biopolymers in subcritical water. J. Supercrit. Fluids. https://doi.org/10.1016/j.supflu.2007.09.037.

Sawant, S.S., Salunke, B.K., Kim, B.S., 2018. Consolidated bioprocessing for production of polyhydroxyalkanotes from red algae Gelidium amansii. Int. J. Biol. Macromol. 109, 1012–1018. https://doi.org/10.1016/j.ijbiomac.2017.11.084.

Smith, A.M., Ross, A.B., 2016. Production of bio-coal, bio-methane and fertilizer from seaweed via hydrothermal carbonisation. Algal Res. 16, 1–11. https://doi.org/10.1016/j.algal.2016.02.026.

Sun, Y., Zhang, J.P., Wen, C., Zhang, L., 2016. An enhanced approach for biochar preparation using fluidized bed and its application for H2S removal. Eng. Process. Process Intensif. Chem. https://doi.org/10.1016/j.cep.2016.02.006.

Toor, S.S., Rosendahl, L., Rudolf, A., 2011. Hydrothermal liquefaction of biomass: A review of subcritical water technologies. Energy. https://doi.org/10.1016/j.energy.2011.03.013.

Tůma, S., Izaguirre, J.K., Bondar, M., Marques, M.M., Fernandes, P., da Fonseca, M.M.R., Cesário, M.T., 2020. Upgrading end-of-line residues of the red seaweed Gelidium sesquipedale to polyhydroxyalkanoates using Halomonas boliviensis. Biotechnol. Reports 27. https://doi.org/10.1016/j.btre.2020.e00491.

Wang, T., Zhai, Y., Zhu, Y., Li, C., Zeng, G., 2018. A review of the hydrothermal carbonization of biomass waste for hydrochar formation: Process conditions, fundamentals, and physicochemical properties. Renew. Sustain. Energy Rev. 90, 223–247. https://doi.org/10.1016/j.rser.2018.03.071.

Warren, F.J., Gidley, M.J., Flanagan, B.M., 2016. Infrared spectroscopy as a tool to characterise starch ordered structure - A joint FTIR-ATR, NMR, XRD and DSC study. Carbohydr. Polym. https://doi.org/10.1016/j.carbpol.2015.11.066.

Xu, Q., Qian, Q., Quek, A., Ai, N., Zeng, G., Wang, J., 2013. Hydrothermal carbonization of macroalgae and the effects of experimental parameters on the properties of hydrochars. ACS Sustain. Chem. Eng. 1, 1092–1101. https://doi.org/10.1021/sc400118f.

Zhao, M., Li, B., Cai, J.X., Liu, C., McAdam, K.G., Zhang, K., 2016. Thermal & chemical analyses of hydrothermally derived carbon materials from corn starch. Technol. Fuel Process. https://doi.org/10.1016/j.fuproc.2016.08.002.

Zollmann, M., Robin, A., Prabhu, M., Polikovsky, M., Gillis, A., Greiserman, S., Golberg, A., 2019. Green technology in green macroalgal biorefineries. Phycologia. https://doi.org/10.1080/00318884.2019.1640516.